PHYSICAL REVIEW B **80**, 140414(R) (2009)

# Element-specific probe of Ru magnetism and local structure in $RuSr_2Eu_{1.5}Ce_{0.5}Cu_2O_{10}$

N. M. Souza-Neto, D. Haskel,* and J. C. Lang
*Advanced Photon Source, Argonne National Laboratory, Argonne, Illinois 60439, USA*

O. Chmaissem and B. Dabrowski
*Material Science Division, Argonne National Laboratory, Argonne, Illinois 60439, USA and Department of Physics, Northern Illinois University, DeKalb, Illinois 60115, USA*

I. Felner
*Racah Institute of Physics, The Hebrew University, Jerusalem 91904, Israel*

(Received 26 August 2009; published 28 October 2009)

Element-specific x-ray magnetic circular dichroism measurements at the Ru $L_3$ absorption edge are used to search for the presence of a net Ru ferromagnetic moment in the superconducting state of $RuSr_2Eu_{1.5}Ce_{0.5}Cu_2O_{10}$. A net moment of $0.21\mu_B/Ru$ is observed in zero applied field. Together with a homogeneous Ru local structure probed by x-ray absorption fine-structure measurements, the results unequivocally demonstrate the coexistence of a ferromagnetic component in the magnetically ordered $RuO_2$ planes with superconductivity in the $CuO_2$ planes.

DOI: 10.1103/PhysRevB.80.140414 PACS number(s): 75.25.+z, 74.70.Pq, 61.05.cj

Rutheno-cuprate layered structures $RuSr_2RECu_2O_8$ (Ru-1212) and $RuSr_2RE_2Cu_2O_{10}$ (Ru-1222) (RE=rare earth) have generated significant interest due to the reported presence in the ground state of concomitant long-range magnetic ordering ($T_M$=100–150 K) and high-temperature superconductivity ($T_c$=20–50 K) in alternating $RuO_2$ and $CuO_2$ planes, respectively. In particular, the possibility of magnetic ordering of the weak ferromagnetic (W-FM),[1] or ferromagnetic,[2] type as originally reported based on bulk magnetization measurements, generated additional excitement albeit with some skepticism. This is because the dipolar and exchange fields generated by a FM or W-FM $RuO_2$ layer in proximity to the $CuO_2$ layers could act as pair breakers or prevent singlet-pair formation altogether ($T_M > T_c$), e.g., due to induced splitting of spin-up and spin-down conduction bands. Density functional theory[3] mitigated some of these concerns by showing that these dipolar and exchange fields are weak enough in Ru-1212 that singlet pairing can still occur in the $CuO_2$ layers, albeit with a modulated SC order parameter the nature of which depends on whether the Ru magnetization is parallel or perpendicular to the $RuO_2$ layers.

More recently, efforts have been devoted to the understanding of phase purity, lattice distortions and the true nature of magnetic ordering in Ru-1212 and Ru-1222 structures.[4–8] Phase purity, in particular ruling out the presence of magnetic impurities with similar ordering temperature [such as $SrRuO_3$ (SRO)], is important in order to support assertions of microscopic uniform coexistence of magnetism and superconductivity. Lattice distortions such as rotations of $RuO_6$ octahedra can affect the magnetic structure through spin-orbit coupling (e.g., Dzyaloshinsky-Moriya interactions[9,10]), antisymmetric exchange interactions, or single-ion anisotropy. As per the magnetic structure, both neutron diffraction and x-ray resonant magnetic scattering (XRMS) measurements have now determined that the magnetic ordering in zero applied field is of the antiferromagnetic (AFM) *G* type in the Ru-1212 phase (Ru moments antiparallel in all three crystallographic directions). However, the presence of a FM component within this magnetic structure, as originally implied from magnetization[1,2] and NMR (Ref. 11) data, was observed in only one[12] but no other[5,6] neutron-diffraction measurements, which set an upper limit of $0.1-0.3\mu_B/Ru$ for such FM component. Furthermore, a representation analysis[8] concludes that a net in-plane FM component must be present, albeit compensated due to alternation of moment direction along the *c* axis. Inconsistencies remain as per the exact orientation of the Ru moments in the *G* type AFM phase, with neutrons indicating *c*-axis alignment[5,6] and XRMS (Ref. 8) indicating alignment along the (102) direction. The current understanding of the magnetic structure of Ru-1222 compounds is even more controversial. Recent neutron-diffraction work by Lynn *et al.*[13] on $RuSr_2Eu_{1.2}Ce_{0.8}Cu_2O_{10}$ failed to detect *any* magnetic ordering associated with the rutheno-cuprate structure. Additionally, small-angle neutron-scattering measurements did not observe any signature of a FM component, and some limited magnetic scattering present in this system was attributed to impurity scattering. In contrast, Mclaughlin *et al.*[7] observed clear magnetic scattering in their neutron-diffraction measurements on $RuSr_2Y_{1.5}Ce_{0.5}Cu_2O_{10}$ indicating antiferromagnetic alignment of Ru spins (Ru moments along the *c* axis). The neutron data, however, could not be modeled with a simple *G*-type AFM structure and arguments were put forward in favor of both FM and AFM Ru-Ru coupling being simultaneously present along the c-axis.[7] Neutron diffraction failed to observe a net FM component in Ru-1222 compounds, an upper limit of $\sim 0.3\mu_B/Ru$ set by the experimental sensitivity.

To reconcile the recent neutron and x-ray scattering measurements with the observation of a FM component in magnetization and NMR data, it is therefore of critical importance to determine if a zero-field FM component of magnetization is present in the Ru sublattice and whether this magnetism is intrinsic to the rutheno-cuprate crystal structure as opposed to being associated with impurity phases. To this end, we undertook an x-ray magnetic circular dichroism (XMCD) and x-ray absorption fine-structure (XAFS) study of the local magnetic and chemical structure of Ru ions in $RuSr_2Eu_{1.5}Ce_{0.5}Cu_2O_{10}$ powder samples. XMCD arises from the breaking of time-reversal symmetry associated with the presence of a (net) FM component of magnetization and hence it is ideally suited for probing the existence of such component in rutheno-cuprates (detection limit $\approx 0.01\mu_B$/Ru ion). Unlike magnetometry, the resonant nature of XMCD yields element-specific magnetization so it can be used to probe the Ru magnetization independently from other contributions. In fact, paramagnetic contributions from RE ions dominate the background intensity at the lattice (nuclear) Bragg-peak positions in neutron-scattering experiments limiting the sensitivity for detection of a FM component to $\approx 0.3\mu_B$/Ru ion.[6,7] As per structural homogeneity, XAFS is ideally suited for detection of nanosized impurity phases which may be present but go undetected in diffraction measurements, due to finite-size broadening or high degree of structural disorder. XAFS probes the local structure even in the absence of long-range order and hence can provide a conclusive answer on the question of local structure homogeneity. Specifically, the need to rule out the presence of SRO FM impurities was pointed out early on[2] and this need exacerbated with the detection of SRO impurities in some[13] but not other[7] neutron measurements.

Ceramic samples of Ru-1222 were prepared by mixing prescribed amounts of $Eu_2O_3$, $CeO_2$, $SrCO_3$, CuO, and Ru (powder), pressed into pellet form, and preheated to 950 °C for one day, regrained, and sintered under oxygen at 1050 °C for two days then furnace cooled.[1,4,14] X-ray diffraction measurements of as-grown samples could not detect the presence of impurity phases and magnetization measurements were used to determine magnetic ($T_M$=125 K) and superconducting ($T_c$=21 K) transition temperatures.[14] SRO powder reference samples were prepared as described in Ref. 15. XAFS measurements at the Ru $K$ edge (21.117 keV) were carried out at undulator beamline 4-ID-D of the Advanced Photon Source. Powder samples were mounted on the cold finger of a closed-cycle refrigerator for low-temperature measurements using a transmission geometry. XMCD measurements at the Ru $L_3$ edge (2.838 keV) were carried out at undulator beamline 4-ID-C of the Advanced Photon Source. Measurements were done in polarization switching mode with data also taken for opposite directions of applied magnetic field to check for experimental artifacts. XMCD was collected using total electron yield and fluorescence yield simultaneously. Powder samples were mounted on the variable-temperature insert of a superconducting magnet for low-temperature measurements down to 5 K in magnetic fields up to 4 T applied along the incident wave vector of circularly polarized (CP) photons. Neither beamline delivers CP radiation at the Ru $L_2$ edge (2.967 keV) preventing the application of sum rules analysis.

Figure 1(a), main panel, shows the field dependence of integrated Ru $L_3$ XMCD intensity in the Ru-1222 sample at 5 K (data points) together with superconducting quantum interference device (SQUID) magnetization data on the same sample (lines). The lower-right inset shows raw XMCD data

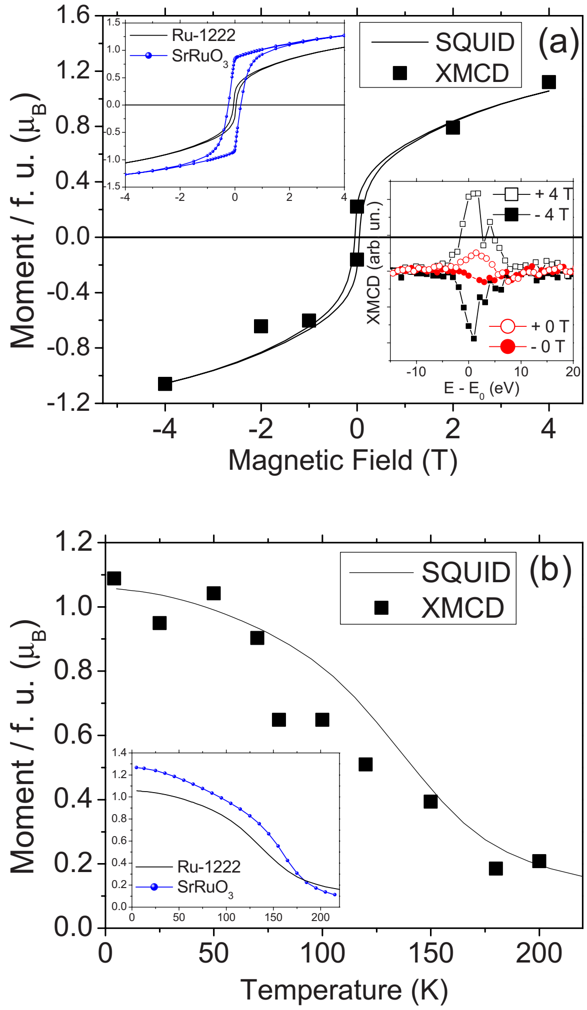


FIG. 1. (Color online) (a) Main panel: magnetic moment per formula unit for Ru-1222 from SQUID magnetometry and (scaled) Ru XMCD data at 5 K (see text). Lower inset: raw XMCD data at 5 K for ±0 and ±4 T fields. Upper inset: SQUID data for SRO and Ru-1222 samples at 5 K. (b) Main panel: SQUID and (scaled) XMCD data for Ru-1222 at 4 T. Inset: SQUID data for Ru-1222 and SRO at 4T.

at 5 K for opposite field directions (0 and 4 T) showing reversal of the XMCD signal upon reversal of the magnetization direction, as expected. The XMCD signal arises from the magnetic ordering of Ru 4$d$ electrons probed by the resonant $2p \rightarrow 4d$ electric-dipole transition. A clear nonzero XMCD signal (FM component) is observed at zero applied field, about 1/5 of its value at 4 T. Since the lack of $L_2$-edge data prevents the application of sum rules to determine the size of the magnetic moments, we used SRO as a reference in order to estimate the magnitude of the FM component in zero-field. SQUID magnetization data on SRO powders (emu/gr) can readily be converted to $\mu_B$/Ru since Ru dominates the magnetization in SRO. By measuring SQUID and XMCD on SRO an arbitrary conversion factor is obtained to place the XMCD data on an absolute magnetization scale. Applying the *same* conversion factor to the XMCD data of Ru-1222 we obtain very good agreement with its SQUID data [see field and temperature dependence in the main panels of Figs. 1(a) and 1(b)], indicating that the Ru FM component dominates the SQUID magnetization data over paramagnetic (rare-earth) contributions and that the nominally different valence state of Ru in SRO ($Ru^{4+}$) versus Ru-1222 (Ref. 16) ($Ru^{4.95+}$) still results in similar Ru XMCD integrated intensity in both samples for a given Ru magnetic moment. This normalization procedure results in a zero-field Ru FM component of $0.21 \pm 0.03 \mu_B$. Note that this magnitude is below the detection limit of neutron-diffraction experiments.[7,13] Additionally, the magnetization is clearly not saturated at 4 T so an ordered FM component of $1.1 \mu_B/\mathrm{Ru}$ at 4 T is consistent with the $1.5(3) \mu_B/\mathrm{Ru}$ local moment found in neutron-diffraction measurements[7] and indicative of a low spin state ($g=2$, $S=1/2$) for $Ru^{5+}$ ions.

After establishing by XMCD that a significant zero-field FM component is present in the Ru sublattice, we used XAFS measurements in order to demonstrate that this component is associated with the Ru-1222 structure and not with impurity phases. Of particular interest is to determine if SRO impurities are present, due to the similarity in magnetic ordering temperature with Ru-1222 [Fig. 1(b)]. The crystal structures of Ru-1222 and SRO are shown in Fig. 2. Although coordination numbers and interatomic distances within the first two coordination shells about Ru atoms are quite similar (Ru-O and Ru-Sr) their local structures are easily distinguishable by XAFS through the different Ru-Ru coordination in the third shell (4 versus 6) and most importantly, through Ru-Cu photoelectron scattering (and related collinear Ru-O(2)-Cu multiple scattering) along the $c$ axis in the fourth coordination shell of the $I4/mmm$ structure of the rutheno-cuprate.[13] A comparison of experimental Fourier-transformed Ru $K$-edge XAFS data for Ru-1222 and SRO at $T=20$ K is shown in the inset of Fig. 3, clearly manifesting these differences in local structure at the higher coordination distances. Quantitative analysis of Ru-1222 XAFS data was carried out using FEFF 6.0 theoretical standards,[17] the scattering amplitudes and phases computed using an 8 Å-sized cluster with lattice parameters and atomic positions from Lynn *et al.*[13] Possible rotations of $RuO_6$ octahedra about the $c$ axis were neglected as these result in a ~0.05 Å splitting between in-plane Ru-O(1) and out-of-plane Ru-O(2) distances, a splitting unresolved with the spatial resolution of our XAFS measurement ($\pi/2k_{\mathrm{max}}=0.12$ Å, where $k_{\mathrm{max}}=13$ Å$^{-1}$ is the largest photoelectron wave number). The radial pair distribution function involving Ru and neighboring atoms within the $R=[1.3,4.0]$ Å region of real space was fitted by including single and multiple-scattering contributions to the XAFS signal. The Fourier transform uses data in the $k=[2,13]$ Å$^{-1}$ range, resulting in 20 independent points in the fitted range.[18] The 12 fitted parameters included distances and bond disorder for Ru-O, Ru-Sr, Ru-Ru, and Ru-Cu single and multiple-scattering paths, as well as an overall correction to the theoretical origin of photoelectron energy ($E_0$ shift) and an amplitude reduction factor to compensate for unaccounted excitations of passive electrons in the theoretical calculation of x-ray absorption.[19] The data were successfully modeled using the known crystal structure (misfit in $R$ space of 2%) with all fitted distances within 0.05 Å of their nominal values. Values for mean-squared bond disorder are in the range of 0.002–0.005 Å$^2$ for Ru-O, Ru-Sr, and Ru-Cu distances, while a larger disorder of 0.012 Å$^2$ for in-plane Ru-Ru distances is likely a result of unaccounted buckling in Ru-O(1)-Ru scattering paths arising from rotations of $RuO_6$ octahedra about the $c$ axis.[13] Fit results are shown in the main panel of Fig. 3. In order to determine if SRO impurities are present in our Ru-1222 sample, we next fitted the data with a linear combination of Ru-1222 and SRO local structures. Since the information content is limited, the structural parameters for SRO were independently determined by fitting the experimental SRO XAFS data, then set in the mixed-phase fits. The fitted fractional content of SRO phase was $2 \pm 5\%$, with the fractional misfit (5%) larger than that of the single-phase fit. While this is not inconsistent with the 7% SRO impurity content reported in neutron-diffraction experiments,[13] it clearly shows that the local structure of Ru ions is predominately homogeneous (>93%) and consistent with the crystal structure of the Ru-1222 phase. In a similar fashion we can also rule out the presence of significant $Sr_2RuO_4$ impurities. We note that our XAFS measurements cannot distinguish between Ru-1222 and Ru-1212 local structures as these are nearly identical (all distances within 0.01 Å).

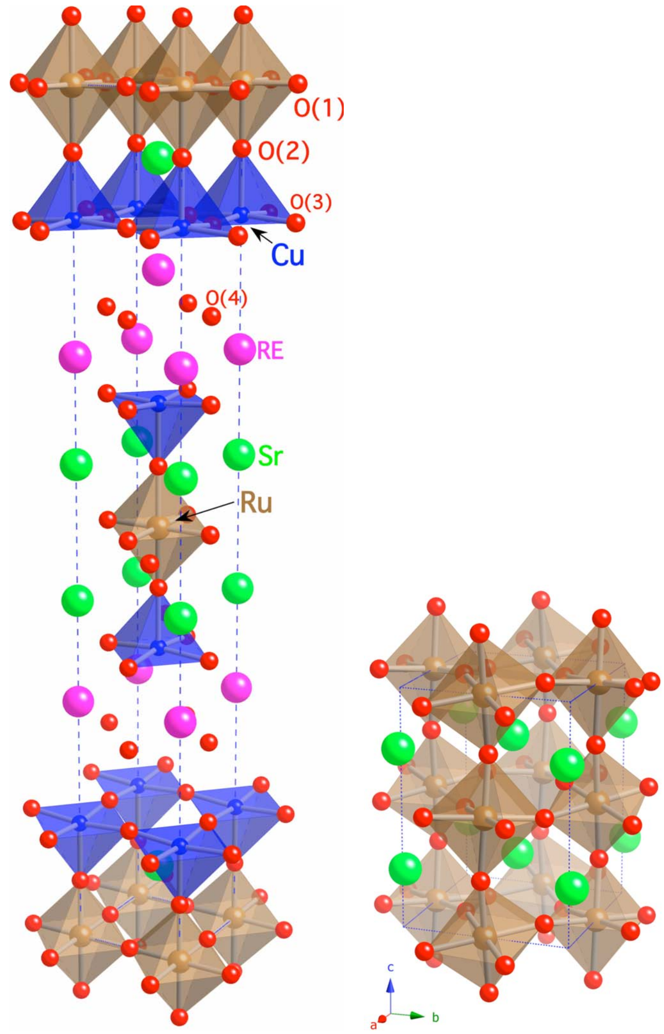


FIG. 2. (Color online) Crystal structure of Ru-1222 (a) and $SrRuO_3$ (b).

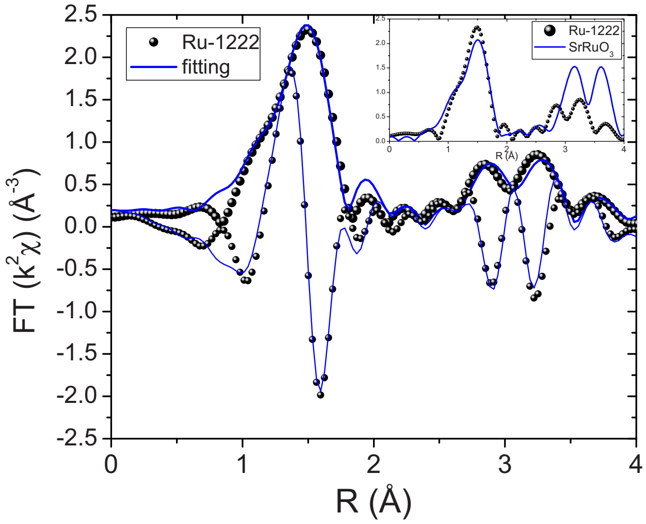


FIG. 3. (Color online) Main panel: Magnitude (large symbols) and real part (small symbols) of complex Fourier transform of XAFS data, together with their respective fits (lines), for Ru-1222 at $T=20$ K. Inset: Magnitude of complex Fourier transform of XAFS data for Ru-1222 and $SrRuO_3$.

In summary, XMCD measurements unequivocally show the presence of a significant zero-field FM component ($0.21\mu_B$/Ru) associated with Ru ions in the Ru-1222 phase (this component is at least ten times larger than expected for a 2% SRO impurity phase $\approx 0.017\mu_B$/Ru). While the magnetically- ordered state in zero field is predominately of the antiferromagnetic type as determined by neutron diffraction,[7] the presence of significant canting or uncompensated Ru spins results in a sizable zero-field FM component in the $RuO_2$ planes. The magnitude of this FM component is below the detection limit of neutron-diffraction measurements, explaining why direct observation was previously not possible in Ru-1222. Our measurements on powders cannot determine the crystallographic orientation of this FM component and the future availability of single crystals should help determine the final details of magnetic ordering. Both the magnitude and orientation of the Ru FM component are important in determining the nature of the spatial modulation in the SC order parameter of Ru-1222.[3] Together with the XAFS finding of an homogeneous local structure at the atomic scale (>93%), the results imply by necessity coexistence of superconductivity and weak ferromagnetism in this hybrid ruthenocuprate structure.

The authors would like to thank D. Keavney and Y.C. Tseng for help with XMCD measurements, Y. Choi, J. Pearson and D. Hinks for help and discussions about SQUID measurements, and M. Onellion for help in obtaining the sample. Work at Argonne is supported by the U.S. Department of Energy, Office of Science, under Contract No. DE-AC-02- 06CH11357. Work at Jerusalem was supported by the Klachky Foundation for Superconductivity. Work at NIU was supported by the NSF (Grant No. DMR-0706610).

*haskel@aps.anl.gov

[1] I. Felner, U. Asaf, Y. Levi, and O. Millo, Phys. Rev. B **55**, R3374 (1997).
[2] J. Tallon, C. Bernhard, M. Bowden, P. Gilberd, T. Stoto, and D. Pringle, IEEE Trans. Appl. Supercond. **9**, 1696 (1999).
[3] W. E. Pickett, R. Weht, and A. B. Shick, Phys. Rev. Lett. **83**, 3713 (1999).
[4] R. Nigam, A. V. Pan, and S. X. Dou, Phys. Rev. B **77**, 134509 (2008).
[5] J. W. Lynn, B. Keimer, C. Ulrich, C. Bernhard, and J. L. Tallon, Phys. Rev. B **61**, R14964 (2000).
[6] O. Chmaissem, J. D. Jorgensen, H. Shaked, P. Dollar, and J. L. Tallon, Phys. Rev. B **61**, 6401 (2000).
[7] A. C. Mclaughlin, I. Felner, and V. P. S. Awana, Phys. Rev. B **78**, 094501 (2008).
[8] B. Bohnenbuck *et al.*, Phys. Rev. Lett. **102**, 037205 (2009).
[9] I. Dzyaloshinsky, J. Phys. Chem. Solids **4**, 241 (1958).
[10] T. Moriya, Phys. Rev. **120**, 91 (1960).
[11] Y. Tokunaga, H. Kotegawa, K. Ishida, Y. Kitaoka, H. Takagiwa, and J. Akimitsu, Phys. Rev. Lett. **86**, 5767 (2001).
[12] H. Takagiwa, J. Akimitsu, H. Kawano-Furukawa, and H. Yoshizawa, J. Phys. Soc. Jpn. **70**, 333 (2001).
[13] J. W. Lynn, Y. Chen, Q. Huang, S. K. Goh, and G. V. M. Williams, Phys. Rev. B **76**, 014519 (2007).
[14] I. Felner, E. Galstyan, and I. Nowik, Phys. Rev. B **71**, 064510 (2005).
[15] B. Dabrowski, O. Chmaissem, P. W. Klamut, S. Kolesnik, M. Maxwell, J. Mais, Y. Ito, B. D. Armstrong, J. D. Jorgensen, and S. Short, Phys. Rev. B **70**, 014423 (2004).
[16] G. V. M. Williams, L.-Y. Jang, and R. S. Liu, Phys. Rev. B **65**, 064508 (2002).
[17] S. I. Zabinsky, J. J. Rehr, A. Ankudinov, R. C. Albers, and M. J. Eller, Phys. Rev. B **52**, 2995 (1995).
[18] E. A. Stern, Phys. Rev. B **48**, 9825 (1993).
[19] J. J. Rehr, E. A. Stern, R. L. Martin, and E. R. Davidson, Phys. Rev. B **17**, 560 (1978).